Preprints of the 21st IFAC World Congress (Virtual)
Berlin, Germany, July 12-17, 2020

A Jump-Markov Regularized Particle Filter for the estimation of ambiguous sensor faults

Enzo Iglésis [*,**] Karim Dahia [*] Hélène Piet-Lahanier [*]
Nicolas Merlinge [*] Nadjim Horri [**] James Brusey [**]

[*] *ONERA DTIS Université Paris Saclay (e-mail: firstname.lastname@onera.fr).*
[**] *Coventry University (e-mail: (E.I) iglesise@uni.coventry.ac.uk; (N.H; J.B) firstname.lastname@coventry.ac.uk)*

Abstract: Sensor or actuator faults occurring on a Unmanned Aerial Vehicle (UAV) can compromise the system integrity. Fault diagnosis methods is then becoming a required feature for those systems. In this paper, the focus is on fault estimation for a fixed-wing UAVs in the presence of simultaneous sensor faults. The altitude measurements of a UAV are commonly obtained from the combination of two different types of sensors: a Global Navigation Satellite System (GNSS) receiver and a barometer. Both sensors are subject to additive abrupt faults. To deal with the multimodal nature of the faulty modes, a Jump-Markov Regularized Particle Filter (JMRPF) is proposed in this paper to estimate the barometric altitude and GNSS altitude measurement faults, including the case when both faults occur simultaneously. This method is based on a regularization step that improves the robustness thanks to the approximation of the conditional density by a kernel mixture. In addition, the new jump strategy estimates the correct failure mode in 100 % of the 100 simulations performed in this paper. This approach is compared with an Interacting Multiple Model Kalman Filter (IMM-KF) and the results show that the JMRPF outperforms the IMM-KF approach, particularly in the ambiguous case when both sensors are simultaneously subject to additive abrupt faults.

Keywords: fixed-wing UAVs, fault estimation, Jump-Markov Regularized Particle Filter, IMM-KF.

1. INTRODUCTION

Sensor faults have a direct impact on the Guidance Navigation and Control (GNC) loop of a Unmanned Aerial Vehicles (UAVs). If faulty information is used by the UAV GNC loop this could compromise the mission of the UAV. Thus Fault Detection, Isolation and Recovery (FDIR) is essential in large UAVs because of their high reliability requirements and increasingly essential to small UAV because of the lack of direct sensor redundancies to reduce costs and the trend towards higher levels of autonomy.

Typical faults are described by Varga (2017) and can be categorized into: time and shape related fault types. Time-related faults can be *persistent* or *intermittent.* Shape-related faults can be *abrupt* (sudden) and *incipient* (gradual build-up).

Various fault detection approaches were presented in the literature. Data-driven approaches (see Ding (2014)) require the use of a large dataset for statistical analysis. However, when the amount of available data is small, model-based approaches (see Ding (2008)) are preferred. Model-based approaches use the knowledge of plant models to provide analytical redundancy. In the case of a fixed-wing UAV, the laws governing the flight dynamics are known (see Beard and McLain (2012); Cook (2012)) allowing the use of model-based approaches.

Several ways to reach the model-based framework were developed. The general idea in this framework, for fault detection, is to compute the error between the actual and predicted measurements, called the residual. Predicted measurements are frequently computed by a state estimator, which may be a Kalman filter. Fault detection is usually performed through statistical tests on residuals. These tests aim to detect a significant change of the residual value. The simplest one consists of a direct comparison of the residual value to a given threshold, but others are based on an assumption about the residual distribution (see Basseville et al. (1993)), such as the Student t-test, the CUmulative SUM (CUSUM), a likelihood ratio test such as the Generalize Likelihood Ratio Test (GLRT), or the Sequential Probability Ratio Test (SPRT). The combined fault detection and isolation is the basis of fault diagnosis.

Fault estimation represents the next level of complexity in fault diagnosis and addresses the reconstruction of fault signals from the available measurements (see Varga (2017)). For fault estimation, a state estimator such as the Kalman filter could be used, or a more sophisticated method may consist of using a bank of Kalman type filters and enclosing it in an Interacting Multiple Model (IMM) architecture (see Zhang and Li (1998); Rago et al. (1998)), which is a widely used state-of-the-art approach. Each filter is associated with nominal or faulty dynamics. These filters interact to provide a global likelihood. However, the

IMM with Kalman Filters (IMM-KF) can diverge in a multimodal case and has the limitations associated with the use of Kalman filters (linear system, Gaussian noise, ...).

The measurement equation considered in this paper used by the fault estimator algorithm has a redundant term that is distinguishable by the sensor noise only. When an additive fault occurs on one of this terms, a multimodality appears on the associated estimated state. Monte-Carlo and particle-based methods were introduced to tackle non-linear and multimodal problems (see Arulampalam et al. (2002)). Moreover, a faulty and a fault-free situation can be considered as a discrete state of the system, like a jump Markov system. Doucet et al. (2001); Tafazoli and Sun (2006) have coupled the Jump Markov Linear System (JMLS) with the particle filter. This approach is used in this paper with a regularized particle filter (see Musso et al. (2001)) to handle the multimodal fault estimation problem better than linearized-Gaussian approaches (like the IMM-KF). It is based on two improvements:

- A regularization step: the particles are drawn from a continuous density rather than a sampled distribution. This yields a better robustness and accuracy.
- A new jump strategy: the a priori distribution of the fault accounts for the filter innovation, which makes it possible to move the particles towards the correct faulty mode.

Compared to conventional fault estimation methods, the Jump-Markov Regularized Particle Filter (JMRPF) introduced in this paper for fault estimation is more robust. Indeed in conventional estimation approaches such as Kalman filter or particle filter, the process noise of the fault estimate must be artificially inflated to detect additive faults with a large magnitude without any guarantee of stability. While, the JMRPF approach allows the estimator to fit the process noise with the knowledge of the state dynamics. The jump process enables to reach any magnitude of an abrupt fault. Therefore, this allows to accurately estimate a fault of any magnitude. In this paper, the JMRPF approach is applied to a fixed-wing UAV with an ambiguous measurement equation (i.e., a non injective measurement equation).

The paper is organized as follows. Section 2 describes the problem. One of the issues addressed by this paper is to detect when a fault occurs, which sensors are responsible; and perform a fault estimation by reconstructing the faults as an additive input signal. In Section 3, the Jump-Markov Regularized Particle Filter approach is introduced for fault estimation. Section 4 details the model used for the simulation. In Section 5, the fault detection and estimation algorithms are evaluated using a Monte-Carlo numerical simulation analysis. Section 6 concludes the paper.

2. PROBLEM STATEMENT

In this paper, a model-based approach will be used to detect and estimate UAV sensor faults and allow for a probabilistic transitioning between a normal operation mode and faulty sensor modes. Fast and accurate fault estimation together with an accurate state estimation algorithm will be necessary to avoid compromising the UAV mission integrity. The case where different types of sensors are used to observe the same state variable is considered here. Here, the altitude of the aircraft is observed using barometer and GNSS altitude measurements. The use of multiple sensors to measure the same variable is what makes the measurement equation ambiguous in a faulty situation. Indeed, only the sensor noise parametrisation makes it possible to differentiate between the observations. Fig. 1 shows the situation where two sensors with different noise standard deviations are used to estimate a state x. The measurements y_1 produced by the first sensor are faulty whereas the measurement y_2 from the second sensor are fault-free. The state estimation of x is based on the conditional density of $p(x|Y_{1:k})$ after updating the predicted conditional density $p(x|Y_{1:k-1})$, where $Y_{1:k}$ is all the measurements of both sensor from time step 1 to k. In this situation, basing our decision on the conditional density $p(x|Y_{1:k})$ highlights the fact that there is an ambiguous choice to decide which mode of the conditional density corresponds to the state estimate. In this paper, this is called an ambiguous sensor fault.

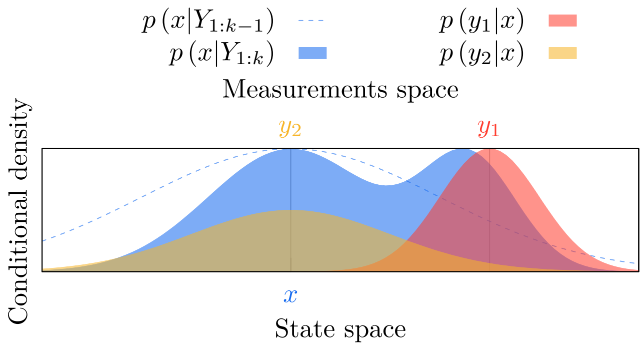

Fig. 1. State estimates of x with a fault-free and faulty measurement estimate density

2.1 Jump-Markov linear system model

The discrete state space model of the Jump-Markov Linear System (JMLS) based on Svensson et al. (2014) is given by:

$$\begin{cases} m_{k+1} \sim p(m_{k+1}|m_k) & \text{(1a)} \\ x_{k+1} = A_{m_k} x_k + B_{m_k} u_k + w_k & \text{(1b)} \\ y_k = C_{m_k} x_k + D_{m_k} u_k + v_k & \text{(1c)} \end{cases}$$

Where m_k is a discrete mode of the system at time step k. The probability to switch from a mode $m^{(i)}$ to $m^{(j)}$ is denoted by $\pi_{ji} = \mathbb{P}\left(m_{k+1}^{(j)}|m_k^{(i)}\right)$. The π_{ji} is an entry of the Π matrix, where i is the row index and j the column index. The vector $x \in \mathbb{R}^{n_x \times 1}$ is the state vector of the system. Each state of the state vector is associated with a Π matrix. The A_{m_k}, B_{m_k}, C_{m_k} and D_{m_k} denotes the usual discrete state space matrices terms, for the mode m_k. In addition to this $y \in \mathbb{R}^{n_y \times 1}$ is the output of the system and $u \in \mathbb{R}^{n_u \times 1}$ is the input. The terms $w_k \in \mathbb{R}^{n_x \times 1}$ and $v_k \in \mathbb{R}^{n_y \times 1}$ denote the process and sensors noise. Because those noise terms are zero mean, the covariance matrices can be defined as $\mathbb{E}\left[w_k w_k^\top\right] = Q_k$ and $\mathbb{E}\left[v_k v_k^\top\right] = R_k$ and they are independent $\mathbb{E}\left[w_k v_k^\top\right] = 0$.

2.2 Jump-Markov linear system for sensor faults estimation

There are two JMLS modes for the fault estimation application. A nominal mode $m^{(0)}$ and faulty mode $m^{(1)}$. The transition probability between each mode is:

$$\Pi = \begin{bmatrix} \pi_{00} & \pi_{10} \\ \pi_{01} & \pi_{11} \end{bmatrix} \tag{2}$$

The probability π_{10} is the probability to switch from nominal to faulty mode while the probability π_{01} is the probability to switch from faulty to be nominal. The π_{ii} entries are the probabilities that the system remain in the same mode. Therefore, $\pi_{00} = 1 - \pi_{10}$ and $\pi_{10} = 1 - \pi_{11}$. To apply this approach to fault estimation, an augmented state space must be considered. Hence ,the extended state vector is given by:

$$x = \begin{bmatrix} z^\top & f^\top \end{bmatrix}^\top \tag{3}$$

Where $z \in \mathbb{R}^{n_z \times 1}$ is the original state vector and $f \in \mathbb{R}^{n_f \times 1}$ is the fault estimates. Only the f vector is associated to a JMLS. Thus, only the states contained in f are associated with a mode $m^{(\cdot)}$. The Markov chain diagram of the JMLS applied to fault estimation is shown in Fig. 2.

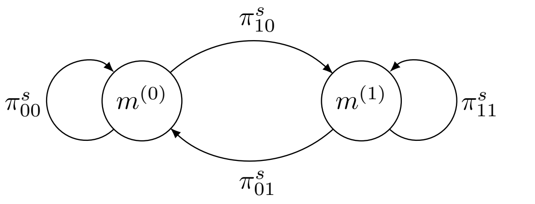

Fig. 2. Markov chain of the JMLS applied to fault estimation for the s^{th} state of state vector f

The state-space matrices in nominal mode are:

$$A_{m^{(0)}} = \begin{bmatrix} A_z & A_{zf} \\ 0_{n_f,n_z} & A_{f,m^{(0)}} \end{bmatrix}, \qquad B_{m^{(0)}} = \begin{bmatrix} B_z \\ 0_{n_f,n_u} \end{bmatrix} \tag{4a}$$

$$C_{m^{(0)}} = \begin{bmatrix} C_z & 0_{n_y,n_f} \end{bmatrix}, \qquad D_{m^{(0)}} = \begin{bmatrix} D_z \\ 0_{n_f,n_u} \end{bmatrix} \tag{4b}$$

Where A_z, B_z, C_z and D_z are the regular matrices associated to the z state vector. The matrix A_{zf} represents the dynamics of the coupling between the fault and the state vector z. Finally $A_{f,m^{(0)}}$ represents the dynamics of the fault of the mode $m^{(0)}$. The state space matrices for the mode $m^{(1)}$ are:

$$A_{m^{(1)}} = \begin{bmatrix} A_z & A_{zf} \\ 0_{n_f,n_z} & A_{f,m^{(1)}} \end{bmatrix}, \qquad B_{m^{(1)}} = \begin{bmatrix} B_z \\ 0_{n_f,n_u} \end{bmatrix} \tag{5a}$$

$$C_{m^{(1)}} = [C_z \ C_f], \qquad D_{m^{(1)}} = \begin{bmatrix} D_z \\ 0_{n_f,n_u} \end{bmatrix} \tag{5b}$$

Where $A_{f,m^{(1)}}$ represents the dynamics of the fault in mode $m^{(1)}$. The matrix A_f can however be the same in mode $m^{(0)}$ and $m^{(1)}$. The unavoidable change is in the matrix $C_{m^{(1)}}$ given the effect of f on the mode $m^{(1)}$ measurement equation with $C_f \in \mathbb{R}^{n_y \times n_f}$ denoting the output matrix of state f:

$$y_{m^{(1)}} = y_{m^{(0)}} + C_f f \tag{6}$$

where $y_{m^{(0)}}$ is the measurement equation for the mode $m^{(0)}$ and $y_{m^{(1)}}$ for the mode $m^{(1)}$. Given that the fault considered here occur on the sensors, the matrices B and D remain unchanged between the mode $m^{(0)}$ and $m^{(1)}$. If fault is considered on a sensor, the entry of C_f associated to the fault estimate of the sensors on the state of f must be set to 1 in order to get an equation measurement of the sensor equal to the nominal equation plus the fault estimate. However it is possible that only one sensor of the f state vector is in mode $m^{(1)}$ and the others are in mode $m^{(0)}$. So in this situation applying the state space of the mode $m^{(0)}$ or $m^{(1)}$ will force all the states of f to be in the mode $m^{(0)}$ or $m^{(1)}$. Then a combination of modes must be considered to assign the states of f in different modes. But being for the s^{th} state of f in mode $m^{(0)} \implies f^s = 0$. Therefore, always applying the state space of the mode $m^{(1)}$ has no effect on fault estimate in mode $m^{(0)}$ and it is the corresponding equations for the fault estimate in mode $m^{(1)}$. Indeed if $f = 0_{n_f}$ then:

$$\begin{cases} x_{k+1,\, m^{(1)}} = x_{k+1,\, m^{(0)}} & \text{(7a)} \\ y_{m^{(1)}} = y_{m^{(0)}} & \text{(7b)} \end{cases}$$

Then on the following sections only the discrete state space model $m^{(1)}$ is used.

2.3 Optimal filtering equation for state estimation

An extended state estimator is needed for fault and state estimation. The state estimator aims to approach the state x_k conditional density at each time-step, given the past measurements $Y_k = [y_1 \ y_2 \ \cdots \ y_k]$. However, an additional issue to the classic state estimation problem is tackled here, since the measurement model is potentially faulty and is therefore unknown a priori. To tackle this issue, the dimension of the estimated parameters is enlarged to $E_k = \begin{bmatrix} x_k^\top & m_k^\top \end{bmatrix}^\top$ in order to estimate both the state x_k and the mode m_k, at each time-step. The modes m_k is a vector associated to the state vector, the value of the mode define if a state is faulty ($m^{(1)}$) or not ($m^{(0)}$). The state conditional density for fault estimation is described by:

$$p(x_k|Y_k) = \sum_{J=0}^{M-1} p(x_k,\, m_k = J|Y_k) \tag{8}$$

where M is the number of modes, and J is the J^{th} n_x-uplet $\begin{bmatrix} m^{(i)}, \ldots, m^{(j)} \end{bmatrix}^\top$, $\forall i, j \in \mathbb{N} \mid [0;\, M-1]$.

The optimal filtering for state estimation consists of two steps: the prediction and the update.

The prediction step aims to predict the state vector $E_{k|k-1}$. Based on the Chapman-Kolmogorov equation the density is propagated as:

$$p(E_k|Y_{k-1}) = \int p(E_k|E_{k-1})\, p(E_{k-1}|Y_{k-1})\, dE_{k-1} \tag{9}$$

Since m_k is independent from x_{k-1} given m_{k-1}, one has:

$$p(E_k|E_{k-1}) = p(x_k|m_k, x_{k-1})\, p(m_k|m_{k-1}) \tag{10}$$

The jump aims to propagate the fault parameters using the following transition density:

$$x_k \sim p(x_k|m_k, x_{k-1}) \tag{11}$$

The update step uses the measurements to update the likelihood from the Bayes rule:

$$p(E_k|Y_k) = \frac{p(y_k|E_k)\, p(E_k|Y_{k-1})}{p(y_k)} \tag{12}$$

3. JUMP-MARKOV REGULARIZED PARTICLE FILTER

To perform the fault estimation, the estimator used in this paper is the regularized particle filter. The particle filter is based on the approximation of this state density by a cloud of particles. The particle filter provides as output the estimated state vector $\hat{x}_k$ and its associated estimated covariance matrix $\hat{P}_k$. The regularization in a particle filter allows a better fit between the theoretical state density and its discrete approximation (see Musso et al. (2001)). Each particle represents a potential state of the system and can be associated with a probability Kernel. The association of a regularized particle filter with a JMLS method is in this paper called a Jump-Markov Regularized Particle Filter (JMRPF). The total number of particles is denoted N_p.

The JMRPF consist of 4 steps: the prediction, the update, the estimation, and the regularization-resampling.

The global algorithm is introduced in Algorithm 1. This algorithm is composed of Algorithm 2, 3, 4 and 5.

Algorithm 1 Jump-Markov Regularized Particle Filter

```
$k \leftarrow 0$
  $\vdots$                                                    ▷ Initialization
loop
    $k \leftarrow k + 1$
    for each $i \in [1,\, N_p]$ do
        PREDICT($x^i_{k|k-1}$, $x^i_{k-1|k-1}$, $m^i_k$, $u_k$, $y_k$)
    end for
    for each $i \in [1,\, N_p]$ do
        UPDATE($\tilde{w}^i_k$, $w^i_{k-1}$, ${x^i}_{k|k-1}$, $u_k$, $y_k$)
    end for
    for each $i \in [1,\, N_p]$ do
        $w^i_k \leftarrow \frac{\tilde{w}^i_k}{\sum_{i=1}^{N_p} \tilde{w}^i_k}$          ▷ Normalize the likelihood
    end for
    ESTIMATE($\hat{x}_{k|k}$, $\hat{P}_{k|k}$, $w_k$, $x_{k|k-1}$)
    $N_{eff} \leftarrow \frac{1}{\sum_{i=1}^{N_p} {w^i_k}^2}$
    if $N_{eff} \leq N_p\Gamma$ then                       ▷ if true then resample
        $\acute{x}_{k|k-1} \leftarrow$MULTINOMIAL($w_k$)              ▷ see (18)
        for each $i \in [1,\, N_p]$ do
            $w^i_k \leftarrow \frac{1}{N_p}$                       ▷ Reset the likelihood
            REGULARIZE($x^i_{k|k-1}$, $\acute{x}^i_{k|k-1}$)
        end for
    end if
end loop
```

Prediction step: In the particle filter, the i^{th} state variable is then propagated using the following transition density:

$$x^i_{k|k-1} \sim p\left(x^i_k | m^i_k, x^i_{k-1}\right) \tag{13}$$

Then, one obtains a predicted cloud of particles ($E^1_{k|k-1}$, $E^2_{k|k-1}, \cdots, E^{N_p}_{k|k-1}$) that makes it possible to approximate $p\left(E_k|Y_{k-1}\right)$

The jump is part of the prediction step. The particles are drawn to jump. The draw is made according to a uniform law and it is compared to the transition density π_{ji}. If a particle is drawn for a jump its new mode is updated. The jump occurs only on the f state vector and its equation is:

$$\tilde{f}^{i,s}_{k|k-1} = \begin{cases} \beta^{i,s}_k & \text{if } U \leq \pi^s_{10} \text{ and } m^{i,s}_k = m^{(0)} \\ f^{i,s}_{k|k-1} & \text{if } U < \pi^s_{11} \text{ and } m^{i,s}_k = m^{(1)} \\ 0 & \text{if } U \leq \pi^s_{01} \text{ and } m^{i,s}_k = m^{(1)} \\ 0 & \text{if } U < \pi^s_{00} \text{ and } m^{i,s}_k = m^{(0)} \end{cases} \tag{14}$$

Where $U \sim \mathcal{U}\left(0,\, 1\right)$ and, $\beta^{i,s}_k$ is an additive fault drawn according to a Gaussian distribution:

$$\beta^i_k \sim \mathcal{N}\left(C_f^\top \tilde{y}^i_k,\, C_f^\top R_k C_f\right) \tag{15}$$

with $\tilde{y}^i_k$ the innovation given by:

$$\tilde{y}^i_k = y_k - \left(C_{m^{(1)}} x^i_{k|k-1} + D_{m^{(1)}} u_k\right) \tag{16}$$

The upper-scripts notation i, s means i^{th} particle and s^{th} state of state vector f with $s \in [1,\, n_f]$. The prediction step is described in Algorithm 2.

Algorithm 2 Detail of the function PREDICT from Algorithm 1

```
function PREDICT($x^i_{k|k-1}$, $x^i_{k-1|k-1}$, $m^i_k$, $u_k$, $y_k$)
    $\eta^i_k \sim \mathcal{N}\left(0,\, Q_k\right)$
    $x^i_{k|k-1} \leftarrow A_{m^{(1)}} x^i_{k-1|k-1} + B_{m^{(1)}} u_k + \eta^i_k$
    for each $s \in [1,\, n_f]$ do                              ▷ Jump step
        $U \sim \mathcal{U}\left(0,\, 1\right)$
        if $m^{i,s}_k = m^{(0)}$ then                     ▷ $f^{i,s}_k$ in mode $m^{(0)}$
            if $U \leq \pi_{10}$ then               ▷ Transition $m^{(0)}$, $m^{(1)}$
                $\tilde{y}^i_k \leftarrow y_k - \left(C_{m^{(1)}} x^i_{k|k-1} + D_{m^{(1)}} u_k\right)$
                $\beta^i_k \sim \mathcal{N}\left(C_f^\top \tilde{y}^i_k,\, C_f^\top R_k C_f\right)$
                $\tilde{f}^{i,s}_{k|k-1} \leftarrow \beta^{i,s}_k$
                $m^{i,s}_k \leftarrow m^{(1)}$
            else                                  ▷ Transition $m^{(0)}$, $m^{(0)}$
                $\tilde{f}^{i,s}_{k|k-1} \leftarrow 0$
            end if
        else if $m^{i,s}_k = m^{(1)}$ then             ▷ $f^{i,s}_k$ in mode $m^{(1)}$
            if $U \leq \pi_{01}$ then               ▷ Transition $m^{(1)}$, $m^{(0)}$
                $\tilde{f}^{i,s}_{k|k-1} \leftarrow 0$
                $m^{i,s}_k \leftarrow m^{(0)}$
            end if
        end if
    end for
end function
```

Update step: In the particle filter, each particle E^i_{k-1} is assigned to a weight w^i_k that is proportional to its likelihood:

$$\tilde{w}^i_k \propto p\left(y_k | m^i_k, x^i_{k|k-1}\right) \tag{17a}$$

$$\tag{17b}$$

However after updating the likelihood of each particle, its weight must be normalized. The Algorithm 3 describes the update step. In this algorithm it is assumed that the likelihood is a Gaussian distribution.

Algorithm 3 Detail of the function UPDATE from Algorithm 1

```
function UPDATE($\tilde{w}_k^i$, $w_{k-1}^i$, ${x^i}_{k|k-1}$, $u_k$, $y_k$)
    $\tilde{y}_k^i \leftarrow y_k - \left(C_{m^{(1)}} x_{k|k-1}^i + D_{m^{(1)}} u_k\right)$    ▷ Innovation
    $\tilde{w}_k^i \leftarrow w_{k-1}^i \Lambda_k^i, \quad \Lambda_k^i = \mathcal{N}\left[\tilde{y}_k^i;\, 0;\, R_k\right]$
end function
```

Estimation step: This step aims to compute a global estimate $\hat{x}_{k|k}$ with its associated covariance matrix $\hat{P}_{k|k}$ based on the likelihood of the particle. This step is described in Algorithm 4.

Algorithm 4 Detail of the function ESTIMATE from Algorithm 1

```
function ESTIMATE($\hat{x}_{k|k}$, $\hat{P}_{k|k}$, $w_k$, $x_{k|k-1}$)
    $\hat{x}_{k|k} \leftarrow \sum_{i=1}^{N_p} w_k^i x_{k|k-1}^i$
    $\hat{P}_{k|k} \leftarrow \sum_{i=1}^{N_p} w_k^i \left(x_{k|k-1}^i - \hat{x}_{k|k}\right)\left(x_{k|k-1}^i - \hat{x}_{k|k}\right)^\top$
end function
```

Regularization-resampling step: This is the last step. It consists of two stages, the resampling and the regularization of the selected particles. Its purpose is to remove the particles with a low likelihood by duplicating the particles with a high likelihood and regularizing the duplicated particles.

Resampling step: The selection of the particles is performed according to a multinomial law with w_k as parameter. Then the probability to choose a particle is:

$$\mathbb{P}\left(\acute{x}_{k|k-1}^i = x_{k|k-1}^j\right) = w_k^j \tag{18}$$

This corresponds to the function MULTINOMIAL(w_k) in Algorithm 1.

Regularization step: For the regularization of the previously selected and duplicated particles, the particles are randomly moved according to a regularization kernel $K(x)$. The regularization is given by:

$$x_{k|k-1}^i = \acute{x}_{k|k-1}^i + hD\varepsilon_k^i \tag{19}$$

where $h \in \mathbb{R}^{+*}$ is the bandwidth factor in the rescaled kernel density $K(\cdot)$ and with $P_k = DD^\top$ and $\varepsilon \sim K(x)$. The kernel density is a symmetric probability density function such that:

$$\int xK(x)\,dx = 0, \quad \int \|x\|^2 K(x)\,dx < \infty \tag{20}$$

The optimal kernel $K(\cdot)$ and bandwidth factor h are those which minimize the Mean Integrated Square Error (MISE) between the hypothetical posterior density and the corresponding regularized empirical representation, defined as:

$$\mathrm{MISE}(\hat{p}) = \mathbb{E}\left[\int \left(\hat{p}(x_k|Y_k) - p(x_k|Y_k)\right)^2 dx_k\right] \tag{21}$$

where $\hat{p}(x_k|Y_k)$ is the particle filter approximation of the state conditional density given by (8). In the case where all particles weight have the same weight, during the resampling step, a suitable choice of the kernel is the bounded Epanechnikov kernel (see Silverman (2018)).

$$K(x) = \begin{cases} \frac{n_x+2}{2c_{n_x}}\left(1 - \|x\|^2\right) & \text{if} \quad \|x\| < 1 \\ 0 & \text{else} \end{cases} \tag{22}$$

where c_{n_x} is the volume of the unit hypersphere in $\mathbb{R}^{n_x}$.

The algorithm of the regularization is described in Algorithm 5.

Algorithm 5 Detail of the function REGULARIZE from Algorithm 1

```
function REGULARIZE($x_{k|k-1}^i$, $\acute{x}_{k|k-1}^i$)
    $\varepsilon \sim K(x)$    ▷ see (22)
    $x_{k|k-1}^i \leftarrow \acute{x}_{k|k-1}^i + hD\varepsilon_k^i$
end function
```

However this regularization-resampling step is not performed at each time step. A criterion is defined to know if a resampling step is needed. The criterion that is used in this paper is the efficiency N_{eff}.

$$N_{\mathit{eff}} = \frac{1}{\sum_{i=1}^{N_p} {w_k^i}^2} \tag{23}$$

If $\frac{N_{\mathit{eff}}}{N_p}$ is lower than user-defined threshold $\Gamma \in (0;\,1)$ then the resampling step is performed.

Finally, after performing all above mentioned steps, the approached conditional density is given by:

$$p(x_k, m_k|Y_k) \approx \sum_{i=1}^{N_p} w_k^i K_h\left(x_k - x_k^i\right)\delta_{m_k^i}(m_k) \tag{24}$$

where:

$$K_h(x) = \frac{1}{h^{n_x}} K\left(\frac{1}{h}x\right) \tag{25}$$

4. LINEAR LONGITUDINAL UAV WITH NAVIGATION AND CONTROL

The system considered in this paper is a linearized longitudinal model of a fixed wing UAV. The state vector representing deviation with respect to the trim point is $z = [p_d\ u\ w\ \theta\ q]^\top$ and $z \in \mathbb{R}^{5\times 1}$ The state p_d is a position in the direction of the vector k^v shown in Fig. 3 representing altitude loos, u is the velocity in direction of the vector i^b shown in Fig. 3, w in direction of the vector k^b axis shown in Fig. 3, θ is the pitch and q to the pitch rate.

The states are partly measured with 5 sensors. The state p_d is directly measured with a GNSS receiver and a barometer, the state u with a pitot tube and the state θ and q with an IMU. The sensors noise is defined by the R_k matrix introduced in the JMLS.

If the fault estimation is performed on the GNSS and barometer measurements only[1], then state vector $f = [f_g\ f_b]^\top$ and $f \in \mathbb{R}^{2\times 1}$, where f_g refers to the GNSS

[1] Similar problem such as speed measurements from pitot tube (airspeed) and GPS (ground speed) could be addressed.

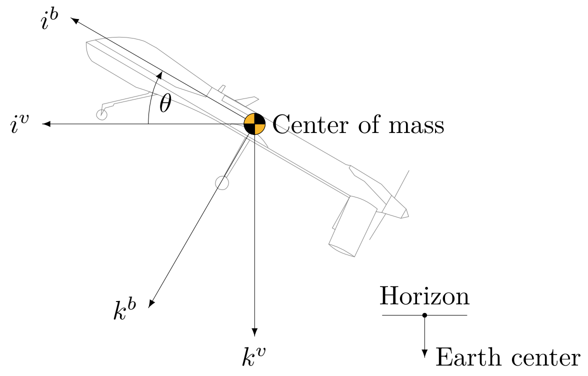

Fig. 3. Fixed wing UAV side view with reference axes for the longitudinal model

altitude fault estimate, f_b to the barometer altitude fault estimate.

The UAV is controlled by a full-state feedback with integrator effect. The block diagram of the control of the UAV is shown in Fig. 4. The C_i gain matrix allows to select the

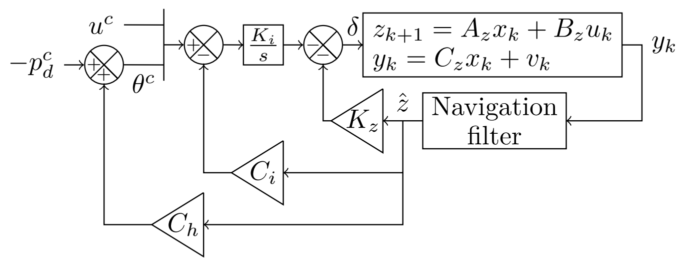

Fig. 4. Block diagram of the control of the UAV

states used for the integrator effect, here θ and u. The C_h gain matrix allows to select the states used for the altitude regulation, here p_d. The gain K_z is the gain of the full-state feedback and K_i is the integral gain. The reference output is $-p_d^c$, u^c and θ^c where θ_c is the desired pitch command defined by $-p_d^c$ the desired altitude and u_c is the speed command. The navigation filter return the state estimate $\hat{z}$ of the z state vector.

Because the model is linearized, an input of 0 refers to the trim condition. The UAV control input vector is $\delta = [\delta_e \ \delta_t]^\top$ where δ_e is the elevator deflection and δ_t is the throttle.

5. SIMULATION RESULTS

To characterize the performances of the JMRPF, numerical simulations were performed with a JMRPF implemented on MATLAB©. The simulation results are compared with an IMM-KF. Even though the system under consideration is linear, there are multi-modalities due to multiple sensor faults modelled in a probabilistic way.

5.1 Numerical parameters of the UAV

A linearized longitudinal UAV model is used. The trim conditions of the linearization are: flight path angle set to 0 rad; straight flight; Altitude set to 500 m; Velocity set to 60 m s^{-1}. The sampling time period used for the simulation analysis is 0.01 s. The simulation parameters used for the UAV dynamics are the following (rounded up to 10^{-3}):

$$A_z = \begin{bmatrix} 1 & 0 & 0.010 & -0.600 & 0 \\ 0 & 0.988 & -0.001 & -0.097 & 0.028 \\ 0 & -0.006 & 0.948 & 0.005 & 0.581 \\ 0 & 0 & 0 & 1.000 & 0.010 \\ 0 & -0.001 & -0.012 & 0 & 0.985 \end{bmatrix}$$
$$B_z = \begin{bmatrix} 0.002 & 0 \\ 0.001 & 0.885 \\ 0.016 & -0.003 \\ -0.005 & 0 \\ -0.963 & 0 \end{bmatrix} \tag{26}$$

The sensors considered for the simulation have an additive white Gaussian noise, the discretized output measurements and sensor error covariance noise matrices are given by:

$$C_z = \begin{bmatrix} -1 & 0 & 0 & 0 & 0 \\ -1 & 0 & 0 & 0 & 0 \\ 0 & 1 & 0 & 0 & 0 \\ 0 & 0 & 0 & 1 & 0 \\ 0 & 0 & 0 & 0 & 1 \end{bmatrix}, \quad D_z = 0_{n_y,n_u}$$
$$R_k = \begin{bmatrix} 5^2 & 0 & 0 & 0 & 0 \\ 0 & 1^2 & 0 & 0 & 0 \\ 0 & 0 & 1^2 & 0 & 0 \\ 0 & 0 & 0 & 0.02^2 & 0 \\ 0 & 0 & 0 & 0 & 0.002^2 \end{bmatrix} \tag{27}$$

The fault estimate is performed on the ambiguous measurements equation on the GNSS and the barometer. Then the corresponding output matrix of the fault estimate is:

$$C_f = \begin{bmatrix} 1 & 0 & 0 & 0 & 0 \\ 0 & 1 & 0 & 0 & 0 \end{bmatrix}^\top \tag{28}$$

and the fault estimate state vector is $f = [f_g \ f_b]$.

The numerical parameters of the control are the following:

$$C_x = \begin{bmatrix} 0 & 0 & 0 & 1 & 0 \\ 0 & 1 & 0 & 0 & 0 \end{bmatrix}, \quad K_i = \begin{bmatrix} 0 & 22.361 \\ -1 & 0 \end{bmatrix}$$
$$K_z = \begin{bmatrix} 0 & 0 & 0.012 & -4.846 & -0.281 \\ 0 & 0.998 & 0 & 0 & 0 \end{bmatrix} \tag{29}$$
$$C_h = [1 \ 0 \ 0 \ 0 \ 0]$$

5.2 Simulation parameters of the JMRPF

The JMRPF parameters are:

$$A_{zf} = 0_{n_z,n_f}, \ A_{f,m^{(0)}} = A_{f,m^{(1)}} = 0_{n_z,n_f} \tag{30}$$

The standard deviation vector used to compute the covariance matrix $P_0 = \text{diag}(\sigma_0)^2$ is equal to:

$$\sigma_0 = [10 \ 2 \ 2 \ 0.1 \ 0.01 \ 25 \ 5]^\top \tag{31}$$

The standard deviation vector used to compute the covariance matrix $Q_k = \text{diag}(\sigma_Q)^2$ is equal to:

$$\sigma_Q = [1 \ 1 \ 1 \ 0.02 \ 0.002 \ 0.08 \ 0.08]^\top \tag{32}$$

For all the parameters of the f state vector the Π matrix [2] used is the same and defined as:

$$\Pi = \begin{bmatrix} 0.99 & 0.01 \\ 0.01 & 0.99 \end{bmatrix} \tag{33}$$

[2] The observed results are sensitive to the values of the probabilities, especially for the JMRPF. Moreover, it is not easy to specify.

For the resampling step:

$$\Gamma = 0.015, \quad h = 0.3894 \tag{34}$$

The matrix R'_k is the one used in the filter. Here $R'_k = \alpha R_k$, with $\alpha > 1$.

The total number of particles N_p is set to 1000.

5.3 Simulation parameters of the IMM-KF

The IMM-KF (see Zhang and Li (1998)) is based on two Kalman filters. The first Kalman filter is the fault-free model. The second Kalman filter performs the state and fault estimation using the same measurements equation and fault model of the JMRPF. The matrices P_0 and R'_k are the same as those used by the JMRPF. The matrix Q_k has been changed on the IMM-KF for the fault estimates states to get a better result. The standard deviation σ_Q used for the IMM-KF is:

$$\sigma_Q = [1 \;\; 1 \;\; 1 \;\; 0.02 \;\; 0.002 \;\; 5 \;\; 1]^\top \tag{35}$$

The transition probability between the IMM-KF models is equal to the matrix Π defined in (33)

5.4 Flight scenario and results

The desired output is set to 0 (relative to the trim point) for desired altitude and velocity. For the flight scenario, two additive intermittent abrupt faults are considered. The first fault occurs on the GNSS altitude at 30 s with a magnitude of 50 m, the fault is deactivated at 50 s. The second fault occurs on the barometer altitude at 40 s with a magnitude of 30 m, the fault is deactivated at 60 s. No fault occurs on the other sensors. The IMM-KF and JMRPF are both applied to this scenario. The JMRPF is initialized in faulty mode $m^{(1)}$ while the IMM-KF is initialized with a more favourable condition which consist of a weight of 0.5 on both of its models.

The navigation filter of the Fig. 4 is performed by the JMRPF or by the IMM.

The RMSE results of this scenario is shown in Fig. 5. Those results are based on 100 simulations with new measurements and initial states at each simulation. The same measurements were used for the IMM-KF and the JMRPF simulations.

On Fig. 5, a peak occurs at each time a fault is activated or deactivated. this can be explained by the fact that when the fault occurred the fault estimate has not predicted its occurrence and at this time step the gap is near the fault magnitude between the fault estimate and the real fault value.

Fault-free situation: The results of Fig. 5 show that in a fault-free situation after converging or after recovering from faulty situation both RMSE are near 0.

GNSS faulty & barometer fault-free: In Fig. 5 the IMM-KF is good at estimating the fault of the GNSS. But the activation of the fault has affected the fault estimate of the fault-free sensor for the IMM-KF while the RMSE of the JMRPF for the fault-free sensor remains unchanged. In this situation the RMSE of the JMRPF for the barometer is approximately 44 times lower than the RMSE of the IMM-KF and around 1.6 times lower for the GNSS.

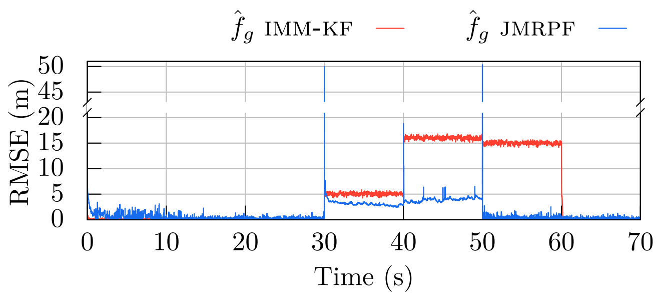

(a) RMSE GNSS fault estimate.

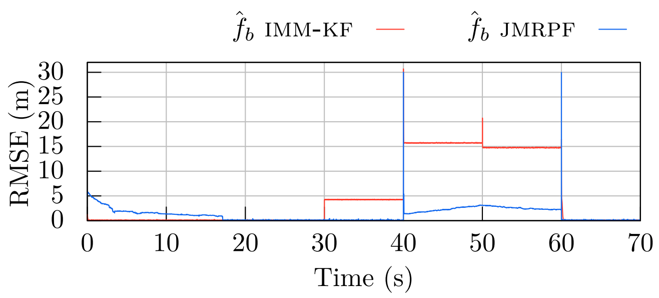

(b) RMSE barometer fault estimate.

Fig. 5. (a) RMSE of the GNSS additive estimated fault. (b) RMSE of barometer additive estimated fault. RMSE are based on 100 simulations.

GNSS faulty & barometer faulty: When both faults are active, the RMSE of JMRPF on the GNSS remains largely unchanged. With the IMM-KF when the second fault is activated, the RMSE of both sensors faults estimates is getting significantly worse. In this situation the RMSE of JMRPF is approximatively 4 times lower than the on of the IMM-KF RMSE for the GNSS and 7 times lower for the barometer.

GNSS fault-free & barometer faulty: The deactivation of one of two faults does not significantly improve the IMM-KF RMSE of the barometer. The RMSE of the JMRPF also remain unchanged for the barometer. However the RMSE of the JMRPF for the GNSS returns to its fault-free value when the fault of the GNSS is deactivated while the RMSE of the IMM-KF for the GNSS is hold to its faulty value. In this situation the RMSE of JMRPF is approximatively 33 times lower than the IMM-KF RMSE for the GNSS and 5.7 times for the barometer.

Based on this RMSE simulation, a mean RMSE for fault estimate state has been computed on each simulation results and sorted. The median simulation results is shown in Fig. 6. The results of Fig. 6 show that the JMRPF seems to not have difficulties to estimate the fault when both faults are activated. On the other hand, the IMM-KF fault estimate of the fault-free sensor is impacted when a fault is active. Moreover, the fault estimate of the barometer estimate only approximately half of the fault. This is believed to be due to the fact that the KF is not suitable for the multimodality that results from using two sensors to estimate one state, while the PF works in the multimodal case.

The impact of the fault estimate on the altitude state p_d of this simulation is shown in Fig. 7.

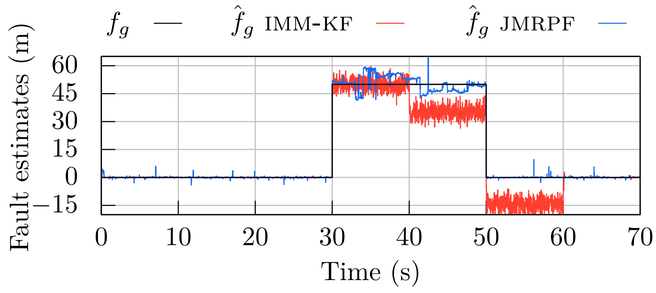

(a) GNSS fault estimates

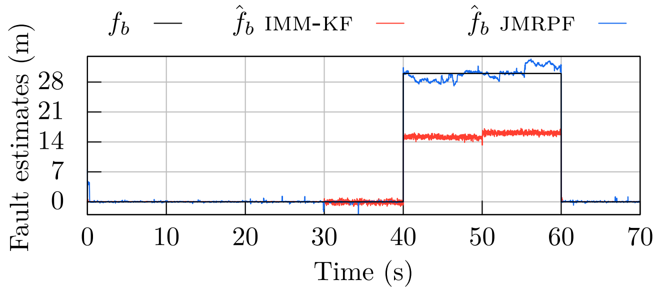

(b) Barometer fault estimates

Fig. 6. GNSS (a) and barometer (b) additive fault estimates Median simulation according to the RMSE results.

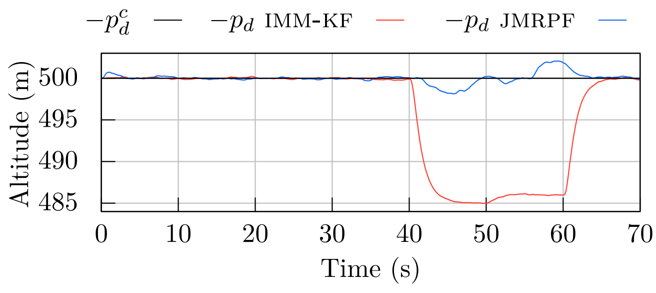

Fig. 7. Altitude of the UAV with the IMM-KF and JMRPF algorithm when a fault occurs on the altitude sensors. Median simulation according to the RMSE results.

Fig. 7 shows that poor quality of the barometer fault estimate of the IMM-KF. With the JMRPF, the error on the barometric altitude estimate is not negligible but significantly lower. This significant change of the UAV altitude can lead to a critical situation for the UAV and mission integrity. The impact of the GNSS fault estimation error is less significant, because the GNSS measurements are noisier than the barometer measurements and, as a consequence, the filter has less confidence in the GNSS measurements compared to the barometer measurements for the estimation of p_d.

6. CONCLUSION

Even though the IMM-KF is well known to be a highly efficient fault estimator, it shows its limitations in the ambiguous case of simultaneous fault measurements on the same output. This was illustrated in this paper with two altitude measurements from barometric altitude sensor and a GNSS receiver. This limitation is due to the multimodal nature of such ambiguous simultaneous faults and may lead to some critical behaviour of the flight control. To address this problem, the JMRPF introduced in this paper can efficiently estimate simultaneous additive abrupt faults assuming knowledge of the likely faults' dynamics.

The application of JMRPF algorithm to a UAV shows that even with intermittent faulty measurements from both altitude sensors, accurate estimation of UAV states is possible.

REFERENCES

Arulampalam, M.S., Maskell, S., Gordon, N., and Clapp, T. (2002). A tutorial on particle filters for online nonlinear/non-gaussian bayesian tracking. *IEEE Transactions on Signal Processing*, 50(2), 174–188.

Basseville, M., Nikiforov, I.V., et al. (1993). *Detection of abrupt changes: theory and application*, volume 104. Prentice Hall Englewood Cliffs.

Beard, R.W. and McLain, T.W. (2012). *Small unmanned aircraft: Theory and practice*. Princeton university press.

Cook, M.V. (2012). *Flight dynamics principles: a linear systems approach to aircraft stability and control*. Butterworth-Heinemann.

Ding, S.X. (2008). *Model-based fault diagnosis techniques: design schemes, algorithms, and tools*. Springer Science & Business Media.

Ding, S.X. (2014). *Data-driven design of fault diagnosis and fault-tolerant control systems*. Springer.

Doucet, A., Gordon, N.J., and Krishnamurthy, V. (2001). Particle filters for state estimation of jump markov linear systems. *IEEE Transactions on signal processing*, 49(3), 613–624.

Musso, C., Oudjane, N., and Le Gland, F. (2001). *Improving Regularised Particle Filters*, 247–271. Springer New York, New York, NY.

Rago, C., Prasanth, R., Mehra, R.K., and Fortenbaugh, R. (1998). Failure detection and identification and fault tolerant control using the imm-kf with applications to the eagle-eye uav. In *Proceedings of the 37th IEEE Conference on Decision and Control*, volume 4, 4208–4213.

Silverman, B.W. (2018). *Density estimation for statistics and data analysis*. Routledge.

Svensson, A., Schön, T.B., and Lindsten, F. (2014). Identification of jump markov linear models using particle filters. In *53rd IEEE Conference on Decision and Control*, 6504–6509. IEEE.

Tafazoli, S. and Sun, X. (2006). Hybrid system state tracking and fault detection using particle filters. *IEEE Transactions on Control Systems Technology*, 14(6), 1078–1087.

Varga, A. (2017). *Solving Fault Diagnosis Problems: Linear Synthesis Techniques*, volume 84. Springer.

Zhang, Y. and Li, X.R. (1998). Detection and diagnosis of sensor and actuator failures using imm estimator. *IEEE Transactions on aerospace and electronic systems*, 34(4), 1293–1313.